

# Site distribution and aliasing effects in the inversion for load coefficients and geocenter motion from GPS data

Xiaoping Wu, Donald F. Argus, Michael B. Heflin, Erik R. Ivins, and Frank H. Webb

Jet Propulsion Laboratory, California Institute of Technology, Pasadena, California, USA

Received 23 September 2002; revised 12 November 2002; accepted 25 November 2002; published 27 December 2002.

[1] Precise GPS measurements of elastic relative site displacements due to surface mass loading offer important constraints on global surface mass transport. We investigate effects of site distribution and aliasing by higher-degree ( $n \geq 2$ ) loading terms on inversion of GPS data for  $n = 1$  load coefficients and geocenter motion. Covariance and simulation analyses are conducted to assess the sensitivity of the inversion to aliasing and mismodeling errors and possible uncertainties in the  $n = 1$  load coefficient determination. We found that the use of center-of-figure approximation in the inverse formulation could cause 10–15% errors in the inverted load coefficients.  $n = 1$  load estimates may be contaminated significantly by unknown higher-degree terms, depending on the load scenario and the GPS site distribution. The uncertainty in  $n = 1$  zonal load estimate is at the level of 80–95% for two load scenarios. **INDEX TERMS:** 1243 Geodesy and Gravity: Space geodetic surveys; 1223 Geodesy and Gravity: Ocean/Earth/atmosphere interactions (3339); 1645 Global Change: Solid Earth; 3260 Mathematical Geophysics: Inverse theory.

**Citation:** Wu, X., D. F. Argus, M. B. Heflin, E. R. Ivins, and F. H. Webb, Site distribution and aliasing effects in the inversion for load coefficients and geocenter motion from GPS data, *Geophys. Res. Lett.*, 29(24), 2210, doi:10.1029/2002GL016324, 2002.

## 1. Introduction

[2] The dynamics of the Earth's hydrosphere involves substantial horizontal mass transport on a multitude of time scales. Measurements of the crustal displacements using continuous Global Positioning System (GPS) data from global tracking sites may contain information about both the surface load and the solid Earth response. *Blewitt et al.* [2001] have used a truncated load deformation harmonic series and 5 years of 3-dimensional relative GPS tracking station displacement data collected at 66 sites to invert for  $n = 1$  load coefficients, which are inferred to be driven by significant global annual and semi-annual cycles of inter-hemispherical mass exchanges. The estimated load coefficients correspond to a determination of the motion of the center of mass of the total Earth system including load (CM) with respect to the center of figure (CF) of the solid Earth surface (often referred to as geocenter motion).

[3] Such an inverse approach, if accurate, would provide a better alternative to the direct GPS observation of the CM motion with respect to the center of GPS tracking network (CN) using orbital dynamics, which is limited by uncertain-

ties in the GPS orbit determination. It would also be useful for monitoring geocenter motions induced by ocean tide loading and by secular surface mass transport. The latter would provide additional and important constraints on the causes and modes of a number of related issues such as sea-level rise, global ice mass balance, etc. However, the GPS site displacements also contain a full array of  $n \geq 2$  deformation harmonics that are induced by the load [e.g., *Chao and O'Connor*, 1988]. These have been ignored based on the orthogonality of the spherical harmonic functions. The orthogonality argument would be valid if the site distribution were globally dense. However, in practice, GPS site distribution is sparse and geographically uneven. Therefore, higher-degree terms will alias into the  $n = 1$  load coefficients resulting in unmodeled errors. Another potential source of error in the inverse procedure is the approximation of using the motion of the CF to replace the motion of the CN. Our main objective in this paper is to explore and evaluate the sensitivity of the inverted  $n = 1$  load harmonic and corresponding geocenter motion to contaminations by these errors.

## 2. Background

[4] The load induced surface displacement  $\mathbf{s}$ , at a position  $(\theta, \phi)$  can be described, in the center-of-mass of the deformed Earth (without load) reference frame (CE) [*Farrell*, 1972], by the spherical harmonic expansion of the surface load density,

$$\Delta\sigma(\theta, \phi) = \sum_{n=1}^{\infty} \sum_{m=0}^n \sum_{q=c,s} M_{nmq} Y_{nmq}(\theta, \phi), \quad (1)$$

and the load Love numbers as:

$$\mathbf{s} = \frac{4\pi a^3}{M_E} \sum_{n=1}^{\infty} \sum_{m=0}^n \sum_{q=c,s} \frac{M_{nmq}}{2n+1} [h'_n Y_{nmq} \hat{\mathbf{e}}_r + l'_n \partial_{\theta} Y_{nmq} \hat{\mathbf{e}}_{\theta} + l'_n \frac{1}{\sin \theta} \partial_{\phi} Y_{nmq} \hat{\mathbf{e}}_{\phi}], \quad (2)$$

where  $a$  is Earth's radius,  $M_E$  is the Earth's mass,  $M_{nmq}$  is the harmonic coefficient of the surface density of the loading mass,  $Y_{nmq}$  is the real-valued spherical harmonic function normalized with geodetic convention [e.g., *Lambeck*, 1980],  $h'_n$  and  $l'_n$  are the surface load Love numbers, and  $\hat{\mathbf{e}}$  is the unit coordinate vector.

[5] In the CE reference frame, the  $n = 1$  load will cause, in addition to a global pattern of variable site displacements, the CM to shift by:

$$\mathbf{r}_{\text{cm}} = \frac{M_L \mathbf{r}_L}{M_E} = \frac{4\pi a^3}{\sqrt{3} M_E} (M_{11c} \hat{\mathbf{e}}_x + M_{11s} \hat{\mathbf{e}}_y + M_{10c} \hat{\mathbf{e}}_z), \quad (3)$$

where  $M_L \mathbf{r}_L = M_x \hat{\mathbf{e}}_x + M_y \hat{\mathbf{e}}_y + M_z \hat{\mathbf{e}}_z$  is the load moment,  $M_L$  and  $\mathbf{r}_L$  are mass and center of mass of the load, respectively; and the CF to shift by an amount that is equivalent to the global mean surface displacement [Trupin *et al.*, 1992]:

$$\mathbf{r}_{cf} = \frac{4\pi}{\sqrt{3}} \frac{a^3}{M_E} \frac{h'_1 + 2l'_1}{3} (M_{11c} \hat{\mathbf{e}}_x + M_{11s} \hat{\mathbf{e}}_y + M_{10c} \hat{\mathbf{e}}_z). \quad (4)$$

[6] The CE frame is not directly accessible by geodetic systems. Instead, two different displacement vectors can be derived for each site  $i$ . The first is the displacement with respect to the CM:  $\mathbf{s}_i - \mathbf{r}_{cm}$  when the CM is chosen to be the origin of the coordinate system for tracking sites and satellite orbits [e.g., Heflin *et al.*, 1992; Ray, 1999]. These can be averaged to determine the CM motion with respect to the CN (or with respect to a fiducial network [Vigue *et al.*, 1992]). Due to limitations in GPS orbit modeling, this direct determination is noisy. More accurately determined is the relative displacement with respect to the CN:

$$\mathbf{S}_i = \mathbf{s}_i - \bar{\mathbf{s}}, \quad (5)$$

where  $\bar{\mathbf{s}}$  is the average displacement of the network. The relative displacement data have been used and modeled by substituting equation (2), retaining only the  $n = 1$  terms, into equation (5) for  $\mathbf{s}_i$  [Blewitt *et al.*, 2001]. Also, the motion of the CN has been assumed to be indistinguishable from that of the CF, or  $\bar{\mathbf{s}} \approx \mathbf{r}_{cf}$ . The  $n = 1$  load harmonic coefficients have been estimated using the GPS data. The motions of the CM and CF with respect to the CE and geocenter motion  $\mathbf{r}_{cm} - \mathbf{r}_{cf}$  follow from equations (3) and (4).

### 3. Covariance Analysis and Simulation

[7] We first investigate effects of the neglected higher-degree terms in  $\mathbf{s}_i$  on the inversion. Equation (2) up to degree and order 50 is used in modeling  $\mathbf{S}_i = \mathbf{s}_i - \mathbf{r}_{cf}$  due to an annual surface load (also assuming  $\bar{\mathbf{s}} \approx \mathbf{r}_{cf}$ ). The observation equations of the relative GPS site displacement time series can be written, in a symbolic matrix form, as:

$$\mathbf{Y} = \mathbf{H}_x \mathbf{X} + \mathbf{H}_c \mathbf{C} + \Delta, \quad (6)$$

where  $\mathbf{X}$  is the  $n = 1$  load coefficients,  $\mathbf{C}$  is the parameter vector for higher-degree load coefficients  $M_{nmq}$  with  $2 \leq n \leq 50$ .  $\Delta$  is the measurement noise vector. When only  $\mathbf{X}$  is solved for by the least squares method, then the estimate is  $\hat{\mathbf{X}} = \mathbf{M} \mathbf{H}_x^T \mathbf{W} \mathbf{Y}$ , where  $\mathbf{W}$  is the inverse covariance matrix of data noise.  $\mathbf{M} = (\mathbf{H}_x^T \mathbf{W} \mathbf{H}_x)^{-1}$  is the covariance matrix for  $\hat{\mathbf{X}}$  if  $\mathbf{C} = \mathbf{0}$ , and is called the computed covariance. The errors in the estimates due to data noise and the ignored parameters are

$$\Delta \hat{\mathbf{X}} = \mathbf{M} \mathbf{H}_x^T \mathbf{W} (\mathbf{H}_c \mathbf{C} + \Delta). \quad (7)$$

Rows of the matrix  $\mathbf{S}_{xc} = \mathbf{M} \mathbf{H}_x^T \mathbf{W} \mathbf{H}_c$  describe the resulting errors in the corresponding elements of the estimate vector due to unit values in  $\mathbf{C}$ , and is called the sensitivity matrix. Note that the computed covariance and the sensitivity matrices are independent of real data and the value of  $\mathbf{C}$ . If the unestimated parameters are treated as random varia-

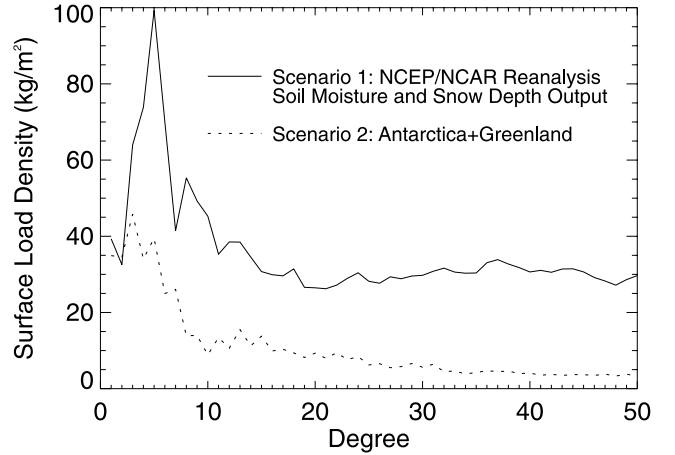


**Figure 1.** Degree root variances of the surface mass density amplitudes (mass per unit surface area) from our scaled annual load variation scenarios.

bles with a covariance matrix  $\Sigma_c$ , then the total covariance (also referred to as ‘consider’ covariance or ‘consider’ uncertainties) for the estimate  $\hat{\mathbf{X}}$  is

$$\mathbf{M}_c = \mathbf{M} + \mathbf{S}_{xc} \Sigma_c \mathbf{S}_{xc}^T. \quad (8)$$

[8] Although various models exist for the annual load variation, it is difficult to assess their quality. To evaluate the ‘consider’ covariance or to perform inverse simulation, we use two annual load scenarios. The load of scenario 1 is caused by the annual soil moisture and snow depth output of the NCEP/NCAR reanalysis [e.g., Chen *et al.* in Ray, 1999]. The  $n = 1$  coefficients are replaced by those of Blewitt *et al.* [2001]. Scenario 2 has uniform Antarctic and Greenland respective winter accumulation and summer melting described by a single cosine term. In both scenarios, the gained and lost mass is assumed to exchange with the world oceans uniformly; and load coefficients  $M_{nmq}$  ( $2 \leq n \leq 50$ ) are scaled by the reported load moment component  $M_z = 4\pi a^3 M_{10c} / \sqrt{3}$  [Blewitt *et al.*, 2001]. The degree root variances of these load coefficients are shown in Figure 1. Significant power can be seen for the higher-degrees. Synthetic GPS annual amplitudes of relative site displacements are generated according to equation (5), with 0.4 mm annual site noise. The square values of the scaled  $M_{nmq}$  are used to construct the diagonal covariance matrices  $\Sigma_c$  for the scenarios.

[9] For illustration, we create a fictitious global GPS network of 132 sites distributed with a  $15^\circ \times 30^\circ$  latitude/longitude grid. The sensitivity matrix is plotted in Figure 2 for the  $n = 1$  sectorial and zonal spherical harmonic load coefficients. These represent the relative aliased errors in the  $n = 1$  load coefficients caused by each same size higher-degree term (e.g., a sensitivity value of 0.1 for  $M_{10c}$  would indicate a 10% error in the estimate of  $M_{10c}$  due to a value of  $M_{nmq} = M_{10c}$ ). The input, inverse recovered values and ‘consider’ uncertainties of the  $n = 1$  coefficients are listed in Table 1 for the two scenarios (columns 2, 3, and 5).

[10] The sensitivity matrix for the 66 site GPS network [Blewitt *et al.*, 2001] is plotted in Figure 3. Here, the uneven

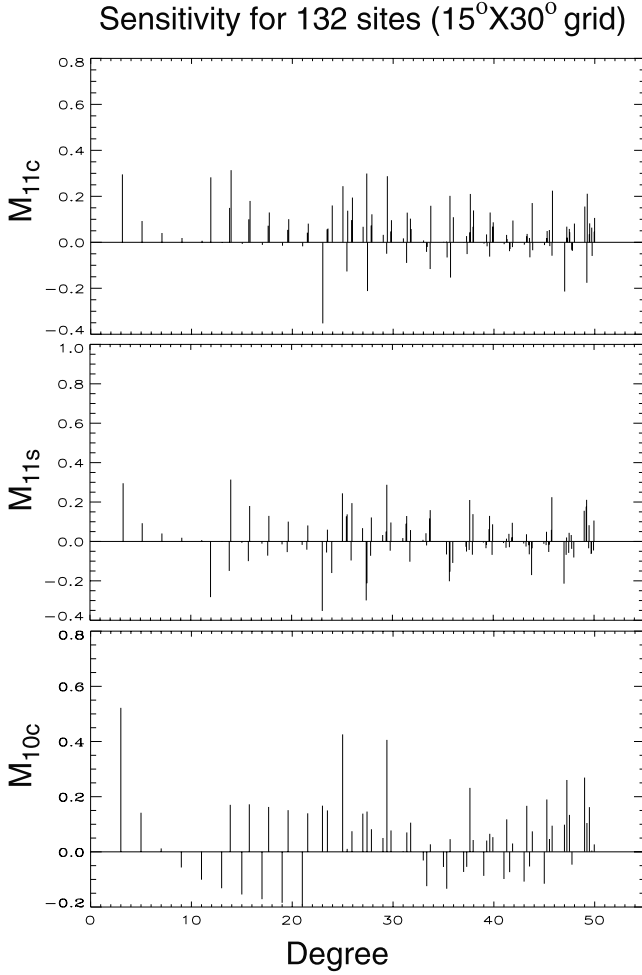


**Figure 2.** Sensitivities of the inverted  $n = 1$  load coefficients to contaminations from unestimated higher-degree load coefficients affecting the GPS data for an ideal GPS network.

site distribution results in a much more complex aliasing pattern with higher magnitudes. The results of the inverse simulation for this network are listed in columns 4 and 6 of Table 1. These suggest that the  $n = 1$  estimates [Blewitt *et al.*, 2001] may be significantly contaminated by the neglected  $n \geq 2$  terms.

[11] Next, we study the effect of approximating  $\bar{\mathbf{s}}$  with  $\mathbf{r}_{\text{ef}}$  in equation (5) for the 66 sites. The differences between CN and CF displacements along X, Y, and Z axes (columns 2–4)

**Table 1.** Inverse Simulation and Covariance Analysis Results

Load	Input kg m <sup>-2</sup>	Inverted		Uncertainty	
		132 sites	66 sites	132 sites	66 sites
$M_{11c}^i$	0.7	1.4	5.2	2.8	12.2
$M_{11s}^i$	14.7	22.9	32.9	6.1	14.0
$M_{10c}^i$	19.4	18.8	13.8	7.1	14.1
$M_{11c}^o$	10.5	12.2	23.4	3.8	24.5
$M_{11s}^o$	-3.9	11.5	8.1	9.7	20.8
$M_{10c}^o$	28.8	32.3	43.2	16.7	27.3
$M_{11c}^{2i}$	-2.2	-1.6	-5.4	1.2	9.4
$M_{11s}^{2i}$	-3.2	-5.3	-8.7	2.9	6.3
$M_{10c}^{2i}$	34.7	67.1	27.3	24.1	27.3

The 2 superscripts in column 1 indicate scenario and in or out-of phase term. e.g.,  $M_{nmq}^{2i}$  means scenario 2, in-phase.

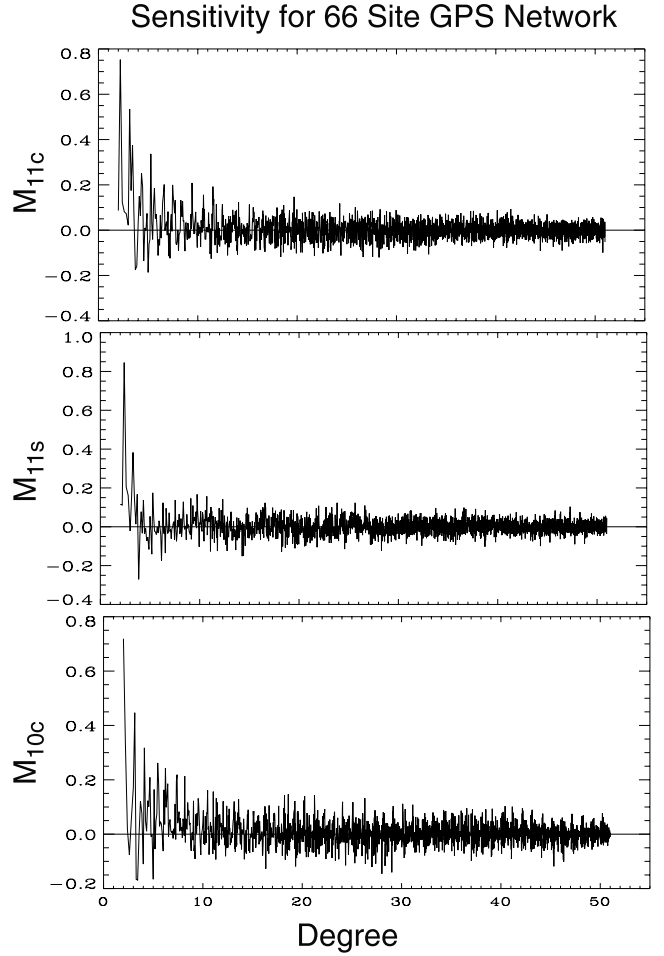


**Figure 3.** Sensitivities of inverted  $n = 1$  load coefficients to contaminations from higher-degree load coefficients. Same as Figure 2 but for the actual geometry of a 66 site GPS network.

are listed in rows 3–5 of Table 2 due to each  $n = 1$  load coefficient (annual amplitude from Blewitt *et al.* [2001]). Using synthetic data (no noise) generated from exact formulation of equation (5) with only  $n = 1$  load and the approximate observation equations, our simulated inversions show 9, 1 and 7% recovery errors for  $M_{11c}$ ,  $M_{11s}$ , and  $M_{10c}$ , respectively, due to the mismodeling. The approximation is unnecessary. Equation (2) can be substituted into both terms in the right-hand-side of equation (5) for load-induced relative displacement obviating the mis-modeling error.

[12] The higher-degree load terms also contribute to the mismodeling error. The network mean displacement due to

**Table 2.** Differences Between Network and Global Mean Displacements

$M_{nmq}$ kg m <sup>-2</sup>	$\bar{\mathbf{s}} - \mathbf{r}_{\text{ef}}$ (mm)		
	X	Y	Z
$M_{11c} = 10.5$	0.139	0.040	-0.098
$M_{11s} = 15.2$	0.060	-0.004	0.041
$M_{10c} = 34.7$	-0.324	0.093	-0.458
$M_{nmq}, n \geq 2$	0.182	0.320	0.487

A value of 34.7 kg m<sup>-2</sup> for  $M_{10c}$  will cause  $r_{cf} = -0.236$  mm and  $r_{cm} = 11$  mm in the Z direction.  $M_{nmq}, n \geq 2$  are from scenario 2.

$2 \leq n \leq 50$  loading terms of scenario 2 is listed in Table 2, row 6, while  $\mathbf{r}_{\text{cf}}$  vanishes without the  $n = 1$  terms. The effect of such mismodeling due to the higher-degree terms is an additional error in the  $n = 1$  load estimate at the 10% level for the loading scenario. Obviously, the effect of CF approximation for CN also depends on the geographical distribution of GPS sites.

#### 4. Discussions and Conclusion

[13] Inversion of relative GPS displacement data for  $n = 1$  loading, and thus geocenter motion, is an interesting proposition to constrain this important geophysical geodetic quantity. The relative GPS displacement data are more precise and relatively less sensitive to orbit errors than are the direct GPS measurements of geocenter displacements. However, the unestimated higher-degree load-induced deformation components contaminate the inversion results for the  $n = 1$  load and geocenter motion. The magnitude of the contamination is a linear function of the higher-degree load components and must be significant since such components are contained in the global annual hydrological cycle [Chao and O'Connor, 1988; Wahr et al., 1998]. The contamination depends on the site distribution and may be more severe when the inverse method is applied to other smaller geodetic networks (GPS/VLBI/SLR/DORIS). The contamination may also be an important factor contributing to the large discrepancy (11 vs. 3.5 mm) between the inverse GPS and direct satellite laser ranging (SLR) annual Z-component geocenter determinations [Blewitt et al., 2001; Bouille et al., 2000], as well as those computed from geophysical models [Dong et al.; Chen et al. in Ray, 1999]. The CF approximation for CN in the inverse introduces non-negligible mis-modeling errors. CN-CF differences also affect other geodetic networks (SLR/GPS/DORIS, particularly small ones) when their direct geocenter results are compared or converted to  $n = 1$  load. For the 30 site SLR network [Bouille et al., 2000], the difference tends to increase the discrepancy mentioned above by  $\sim 1$  mm when the NCEP/NCAR load scenario is used.

[14] The annual surface load we seek to constrain using geodetic data also has atmospheric and internal oceanographic contributions, and is different from the two scenarios. Our 'consider' uncertainties and simulated inverse recovery errors depend on the loading scenario, and thus should be viewed only as order-of-magnitude illustrations. However, since significant higher-degree load components can be expected for the annual surface mass transport cycle,

our sensitivity and uncertainty estimates illuminate the fundamental underdeterminedness of the inverse problem. Without reliable a priori knowledge of the surface load, it is difficult to retrieve all significant harmonics using a sparse and uneven GPS network lacking coverage in the polar areas, oceans, and southern hemisphere. Data now being collected by the GRACE gravity mission will accurately map the annual and semi-annual global surface mass redistribution. The precise GPS relative displacement measurements, as described by equation (5), nonetheless provide additional constraints on new models of time-variable surface mass variations. The  $n = 1$  harmonic, with its very global nature, is an essential part of these variations.

[15] **Acknowledgments.** This work was carried out at the Jet Propulsion Laboratory, California Institute of Technology, under contract with the National Aeronautics and Space Administration. We thank Ben Chao and two other reviewers for comments.

#### References

- Blewitt, G., D. Lavalée, P. Clarke, and K. Nurutdinov, A new global model of Earth deformation: Seasonal cycle detected, *Science*, 294, 2342–2345, 2001.
- Bouille, F., A. Cazenave, J. M. Lemoine, and J. F. Cretaux, Geocenter motion from the DORIS space system and laser data on Lageos satellites: Comparison with surface loading data, *Geophys. J. Int.*, 143, 71–82, 2000.
- Chao, B. F., and W. P. O'Connor, Global surface water-induced seasonal variations in the Earth's rotation and gravitational-field, *Geophys. J. Int.*, 94, 263–270, 1988.
- Heflin, M., W. Bertiger, G. Blewitt, A. Freedman, K. Hurst, S. Lichten, U. Lindqwister, Y. Vigue, F. Webb, T. Yunck, and J. Zumberge, Global geodesy using GPS without fiducial sites, *Geophys. Res. Lett.*, 19, 131–134, 1992.
- Lambeck, K., *The Earth's Variable Rotation*, 449 pp., Cambridge Univ. Press, New York, 1980.
- Farrell, W. E., Deformation of the Earth by surface loads, *Rev. Geophys.*, 10, 761–797, 1972.
- Ray, J., (Eds.), *IERS Analysis Campaign to Investigate Motions of the Geocenter*, IERS Technical Note 25, 121 pp., Central Bureau of IERS, Paris, France, 1999.
- Trupin, A. S., M. F. Meier, and J. M. Wahr, Effects of melting glaciers on the Earth's rotation and gravitational field: 1965–1984, *Geophys. J. Int.*, 108, 1–15, 1992.
- Vigue, Y., S. M. Lichten, G. Blewitt, M. B. Heflin, and R. P. Malla, Precise determination of Earth's center of mass using measurements from the global positioning system, *Geophys. Res. Lett.*, 19, 1487–1490, 1992.
- Wahr, J. M., M. Molenaar, and F. Bryan, Time variability of the Earth's gravity field: Hydrological and oceanic effects and their possible detection using GRACE, *J. Geophys. Res.*, 103, 30,205–30,229, 1998.

D. Argus, M. Heflin, E. Ivins, F. Webb, and X. Wu, Jet Propulsion Laboratory, California Institute of Technology, 4800 Oak Grove Dr. MS 238/600, Pasadena, CA 91109, USA. (Xiaoping.Wu@jpl.nasa.gov)